Transp Porous Med (2014) 105:1–22
DOI 10.1007/s11242-014-0354-z

Experimental Investigations of Natural Convection in Wire-Woven Bulk Kagome

Xiao Hu Yang · Jia Xi Bai · Ki-Ju Kang · Tian Jian Lu · Tongbeum Kim

Received: 9 March 2014 / Accepted: 24 June 2014 / Published online: 8 July 2014

Abstract Natural convection in an open and highly anisotropic cellular material, wire-woven bulk Kagome (WBK) is experimentally characterized. A series of pressure drop and heat transfer experiments are conducted. In particular, effect of inclination angle on the heat transfer rate for porous-cored heat sinks (WBK and metallic foams), as well as smooth plate was experimentally investigated. There exists an optimal inclination angle for smooth plate and porous-cored heat sinks in association with the maximum heat transfer rate (Nusselt number). An advance in optimal inclinational angle was observed in porous media during the full inclination angle range from 0° (horizontal) to 90° (vertical) due to the enhanced lateral conduction and a further advance was found in WBK specimen. A strong anisotropic heat transfer existed in terms of different orientations of WBK specimen: O-B orientation with a bigger cross-sectional surface area density (blockage ratio) reveals a higher heat transfer rate than O-A orientation. Further, in comparison with isotropic metallic foams with a given porosity, the WBK which is positioned at vertical orientation can dissipate more heat than the foams due to the higher permeability resulting from less pressure drop in the WBK formed by an assembly of cylindrical wires.

X. H. Yang (✉)
School of Energy and Power Engineering, Xi'an Jiaotong University, Xi'an 710049, People's Republic of China
e-mail: thomasyangfly@126.com

J. X. Bai · T. J. Lu (✉)
State Key Laboratory for Strength and Vibration of Mechanical Structures, School of Aerospace, Xi'an Jiaotong University, Xi'an 710049, People's Republic of China
e-mail: tjlu@mail.xjtu.edu.cn

K.-J. Kang
Department of Mechanical Systems Engineering, Chonnam National University, Gwangju 500-757, South Korea

T. Kim (✉)
School of Mechanical Engineering, University of the Witwatersrand, Wits, Johannesburg 2050, South Africa
e-mail: tongkim@wits.ac.za

Keywords Wire-woven bulk Kagome · Natural convection · Inclination angle · Experiment

List of Symbols

Variables

A_0	Area of a unit cell subjected to heat input (m^2)
A_s	Cross-sectional area of a ligament (m)
d	Diameter of a circular ligament (m)
f	Inertial coefficient
g	Gravity acceleration (m/s^2)
h	Natural convection heat transfer coefficient W/(m^2K)
H_c	Height of a unit cell (m)
k	Thermal conductivity (W/mK)
K	Permeability (m^2)
L	Characteristic length (m)
Nu	Nusselt number
p	Pressure (Pa)
q''	heat flux (W/m^2)
Ra	Rayleigh number
s	Axis along the tortuous ligament (m)
T	Temperature (K)
u	Velocity (m/s)
U_m	Mean velocity (m/s)
v	Kinetic viscosity (m^2/s)
x, y, z	Cartesian axis direction (m)

Greek Symbols

α	Thermal diffusivity (m^2/s)
β	Thermal expansion coefficient density of air (kg/m^3)
ε	Porosity
ρ	Density (kg/m^3)

Subscripts

av	Average
d	Ligament
e	Effective property
f	Fluid phase
m	Modified
q''	Constant heat flux thermal boundary
s	Solid phase
T	Constant temperature thermal boundary
W	Substrate wall
∞	Ambient of reference
$*$	Relative property

1 Introduction

Highly porous periodic cellular materials (PCMs) that provide novel mechanical and thermal properties have been developed due to their advantages including excellent specific strength and stiffness, and potential for multifunctional applications such as simultaneous load bearing and thermal management over conventional porous media (Evans et al. 2001; Kim et al. 2004a, b). Multiple-layered PCMs with unit cells of pyramid (Zok et al. 2004), octet (Chiras et al. 2002), and Kagome (Hyun et al. 2003) have been introduced, whose fabrication process involves stacking node-to-node single-layered structures and then brazing (Evans et al. 2001). Recently, a new technique for fabricating multi-layered PCMs with Kagome-like unit cells through wire-woven techniques, the so-called "wire-woven bulk Kagome (WBK)", was devised (Kim et al. 2005).

For heat dissipation applications, strong thermal spreading via ligaments and flow mixing by ligaments are preferred to transport the heat more efficiently from heat sources, but typically high pressure drop is accompanied (Evans et al. 2001). Especially for natural convection heat transfer in porous media, the driving force for free fluid flow is the buoyancy force which is greatly influenced by the pressure drop across an inserted porous core. Therefore, the porosity and surface area density of the porous core affect the pressure drop which determines the flow rate of the convective fluid flow and natural convection heat transfer.

Forced convection heat transfer characteristics of the above-mentioned PCMs with tetrahedral lattice (Kim et al. 2005), X-type lattice (Yan 2013), Kagome and WBK cored sandwich panels (Joo et al. 2011; Hoffmann et al. 2003) have been reported. These PCMs are highly aerodynamically anisotropic. Therefore, forced convection heat transfer and pressure drop in these PCMs are strongly dependent on a specific orientation of the PCMs to the direction of coolant flow (Hoffmann et al. 2003; Kim et al. 2005; Joo et al. 2011; Yan 2013). On the other hand, stochastic porous media such as metal foams which are mechanically and aerodynamically isotropic have also shown superior heat removal capacity over non-porous heat dissipation media e.g., fins.

For natural convection, overall heat transfer can be enhanced about 2.4 times by copper (Cu) foams (Qu et al. 2012; Bhattacharya and Mahajan 2006). It has been found that the enhancement was significantly influenced by the effective thermal conductivity and pore size. A higher conductivity and a bigger pore size result in a greater enhancement in natural convection heat transfer. Large surface area density (surface are per unit volume) is associated with such porous media and enhances the overall heat transfer but causes a large pressure drop, reducing the flow rate of the coolant flow induced by the buoyancy forces. Stronger flow mixing and lower pressure drop are closely linked to porosity (or relative density), open flow area ratio, and surface area density. Therefore, a preferable heat dissipation medium keeps a balance between heat transfer (enhanced by increasing the relative density or surface area density) and flow resistance (reduced by decreasing the relative density or flow blockage).

WBK has bigger pores and can be made of highly conducting materials such as aluminum. Furthermore, forced convection results showed that WBK provides lower flow resistance and pressure drop than foams and other PCMs for a given porosity (Joo et al. 2009, 2011). Therefore, it is expected to thermally perform better in natural convection than them. In the present study, a series of steady-state natural convection experiments are conducted with a brazed aluminum (Al) WBK sintered on an Al substrate having the core porosity of $\varepsilon = 0.962$ for Rayleigh number $Ra_{q''}$ ranging from 5.0×10^7 to 2.3×10^8 under constant heat flux. Particular focus is placed on the effects of aerodynamic anisotropy of WBK, which varies

with an inclination of the WBK with respect to the horizontal position on natural convection heat transfer.

2 Experimental Details

2.1 Specimen of a WBK

The WBK core is fabricated by continuous helical wires that are systematically assembled in six directions for multiple WBK layers. This type of fabrication technique is different to that of the existing methods for creating multi-layered truss cellular metals, which are based on stacking node-to-node and bonding of single-layered truss cellular metals. This fabrication method allows the capability of continuous assembling, robustness of truss cores, and mass production (Lee et al. 2007; Kang 2009).

A specimen of a WBK was fabricated as follows. First, wires of aluminum 1100-O with a diameter of 1 mm were formed into a helical shape with a pitch of 14.7 mm and helical radius of 0.6 mm. The helical wires were then assembled in six directions to create multi-layered WBK specimens as shown in Fig. 1. After the wires have been woven, brazed agent was pasted in the helical joints (see Fig. 2).

2.2 Experimentation

Permeability, effective thermal conductivity, and natural convection heat transfer in the WBK sample were measured. To determine the permeability, pressure drop across the WBK was measured in a forced convection test rig (Fig. 3a). The average mass flow rate of convective flow was calculated based on the velocity profiles that were traversed along the channel height H at the mid-width of the channel were traversed using a stagnation probe. The probe was located at the $9D_h$ upstream of the test section where D_h is the hydraulic diameter of a rectangular test channel. A static pressure tapping was flush mounted on the inner channel wall at the same upstream location as the stagnation probe. Pressure readings from both the stagnation probe and the static tapping were recorded by a differential pressure transducer.

To measure the steady-state effective thermal conductivity of WBK samples saturated with air ($k_f = 0.0265$ W/mK), a purposely designed test rig is built as illustrated in Fig. 3b. The WBK specimen is put into a cubic container made of a low conducting material (Perspex 0.18 W/(mK)). A constant heat flux is imposed by an etched-foil heating pad controlled by an AC power supply, on the upper side of the copper plate, ensuring a minimized natural convection of the fluid phase (air) fully saturating the porous core. Hence, heat transferred via the fluid phase in the sample is, therefore, dominated by conduction from the top to the bottom and removed from the test cube (made of a 0.01-m thick-copper plate), with coolant supplied from a cooling system (Contraves Rheotherm 115^{TM}) flowing through wound passages machined into the copper plate. To measure the temperature and net heat flux, T-type thermocouples (Omega^{TM}) and a film-type heat flux gage are separately attached with thermal grease to the lower copper plate. To estimate the heat lost through the test section side walls, two additional T-type film thermocouples are placed on the inner and outer sides of the Perspex side wall.

Figure 3c illustrates schematically the experimental setup for natural convection measurement. The purposely designed test rig, placed in a Plexiglas room, is consisted of wire-woven bulk Kagome sample, power supply system, data acquisition system, and right-angle geom-

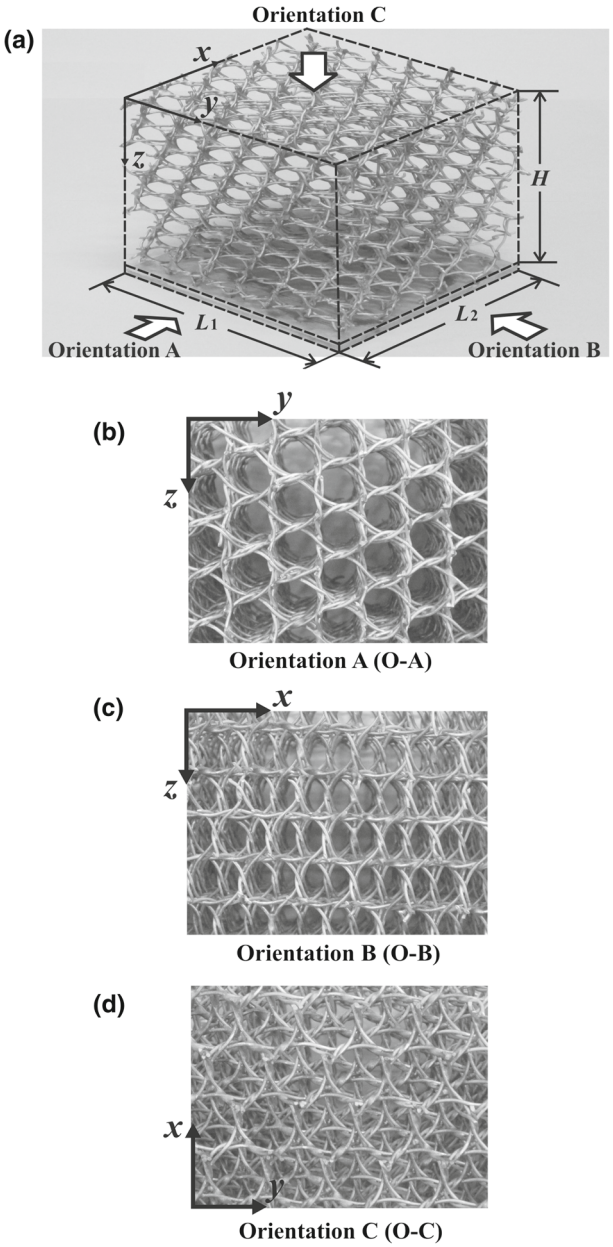

Fig. 1 Photos of wire-woven bulk Kagome (WBK) sample and three typical orientation views

etry support. The WBK sample (O-C orientation) with size of 0.075 m (length) × 0.075 m (width) × 0.05 m (height) (see Fig. 1a) is sintered with a 2-mm thick Al substrate (0.075 m (length) × 0.075 m (width)) with preciously machined grooves for setting up the thermocouples and heat flux gage. To model the typical thermal boundary condition for electronic devices, an electrical film heater with surface area identical to that of the WBK's

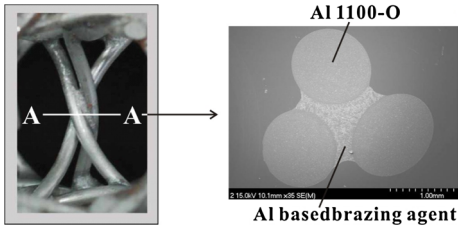

Fig. 2 The brazed details of Al wire-woven bulk Kagome

substrate is attached to the substrate, with its power input controlled by an adjustable DC power supply. To reduce the heat loss from the opposite face of the Al substrate, the substrate is covered with a low conducting polyurethane foam with thermal conductivity of 0.02 W/(mK).

The substrate temperature is estimated by calculating the arithmetic average of the temperatures measured by nine T-type thermocouples fixed in the three grooves, each having 0.75 mm in width and 0.5 mm in depth (see Fig. 3d). The grooves are machined in the substrate with 30-mm interval. The ambient temperature is monitored by another four T-type thermocouples. All the temperatures are monitored and obtained using an Agilent data acquisition system. To investigate the influence of inclination angle, the whole test rig is fixed on a right-angle geometry support whose inclination can be varied continuously from 0° to 180°. The heat flux is adjusted from 519 to 1995 W/m^2 to obtain different Rayleigh numbers and substrate temperatures. The measurements are performed in a big chamber capable of maintaining a stable thermal and fluid surrounding (Fig. 3c). The test data are all obtained under steady-state condition: fluctuations of the average substrate temperature and the temperature difference between the substrate and ambient are restricted to within ±0.2 K during a period of 100 min.

2.3 Data Reduction

2.3.1 Permeability

To quantify the permeability of the present WBK sample, Forchheimer extended Darcy equation (Antohe et al. 1997; Beavers and Sparrow 1969; Joseph et al. 1982; Vafai and Tien 1982) was used as

$$-\frac{\mathrm{d}p}{\mathrm{d}x} = \frac{v_\mathrm{f} u}{K} + \frac{\rho f}{\sqrt{K}} u^2, \tag{1}$$

where $\mathrm{d}p/\mathrm{d}x$ is the pressure drop, u is the velocity, ρ and v_f are the density and kinetic viscosity of the saturating fluid, respectively, and f is the inertial coefficient. Then, the measured pressure drop across the WBK was correlated as a function of the mean flow velocity as

$$\Delta p/\Delta x = au + bu^2 \tag{2}$$

By comparing Eqs. (1) and (2), the permeability K and inertial coefficient f may be written as

$$K = v_f/a \tag{3a}$$

$$f = b\sqrt{K}/\rho \tag{3b}$$

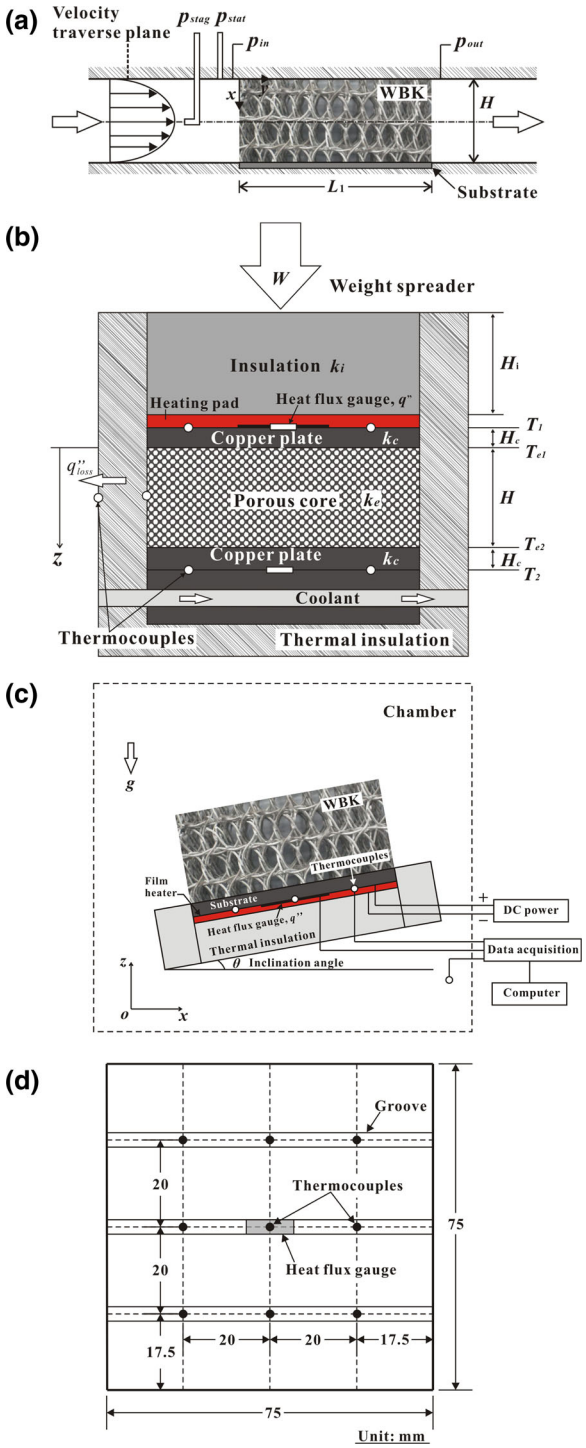

Fig. 3 Schematic of the test facilitates for: **a** permeability measurement; **b** effective thermal conductivity measurement; **c** natural convection heat transfer measurement: **d** locations of thermocouples

2.3.2 Effective Thermal Conductivity

To measure the effective thermal conductivity of WBK specimen saturated with air (k_f = 0.0265 W/mK), steady-state heat conduction measurement was conducted. The surface temperatures T_1 and T_2 are separately measured by K-type thermocouples built-in the film heat flux gage (Omega^{TM}), as well as T-type foil thermocouples (thickness 13 μm, Omega^{TM}) attached to the copper plates. As illustrated in Fig. 3b, one-dimensional heat conduction occurs along the z-axis. The effective thermal conductivity k_e of the test sample is calculated by following Fourier's steady-state heat conduction law.

$$k_e = -\frac{q''_{net} H}{\Delta T}, \tag{4}$$

where q''_{net} is the net heat flux defined as $q''_{net} = q''_{input} - q''_{loss}$, H is the sample height along the z-axis Fig. 3b and $\Delta T = T_{e2} - T_{e1}$ is the temperature difference between the upper and lower surfaces of the sample, estimated as

$$T_{e2} = T_2 + \frac{q''_{net} H_c}{k_c} \tag{5a}$$

$$T_{e1} = T_1 - \frac{q''_{net} H_c}{k_c} \tag{5b}$$

Here, T_2 and T_1 are the temperatures of the lower and upper surface of the copper (substrate) plate directly measured by the attached thermocouples.

2.3.3 Heat Transfer Rate

For the quantitative evaluation of the thermal performance of the WBK, the average Nusselt (Nu_{av}) and Rayleigh ($Ra_{q''}$) numbers are adopted. The Nu_{av} number is defined as

$$Nu_{av} = \frac{h_{av} L}{k_f}, \tag{6}$$

where L is a characteristic length (L_1 selected for the present study) and k_f is the thermal conductivity of fluid phase (air). The average natural convective heat transfer coefficient h_{av} is defined as

$$h_{av} = \frac{q''}{T_w - T_\infty}, \tag{7}$$

where q'' is the heat transfer rate of natural convection in the WBK, while T_w and T_∞ are the temperatures of the heated substrate and the ambient air obtained by averaging the readings of nine thermocouples embedded in the substrate and distributed in the chamber (four thermocouples), respectively.

The Rayleigh ($Ra_{q''}$) number is defined as

$$Ra_{q''} = \frac{g\beta q'' L^4}{\alpha_f \nu_f k_f}, \tag{8}$$

where g is the gravitational acceleration; L is the characteristic length while β, α_f, ν_f, and k_f are the coefficients of thermal expansion, thermal diffusivity, kinematic viscosity, and thermal conductivity of air. Relevant thermo-physical properties in Nu_{av} and $Ra_{q''}$ are evaluated at the characteristic temperature $(T_w + T_\infty)/2$.

2.4 Measurement Uncertainties

2.4.1 Permeability

The estimate of measurement uncertainty associated with permeability, K is very crucial. The pressure gradient is governed by the constant a at lower velocities and by b at higher velocities in Eq. (2). Antohe et al. (1997) proposed a method to accurately quantify permeability K obtained by the method of least-squares regression. The both constants a and b in Eq. (2) are determined as (Montgomery 1997):

$$a = \frac{\sum U_i \Delta p_i \sum U_i^4 - \sum U_i^3 \Delta p_i \sum U_i^3}{\sum U_i^2 \sum U_i^4 - \left(\sum U_i^3\right)^2} \tag{9a}$$

$$b = \frac{\sum U_i^2 \Delta p_i \sum U_i^2 - \sum U_i \Delta p_i \sum U_i^3}{\sum U_i^2 \sum U_i^4 - \left(\sum U_i^3\right)^2}, \tag{9b}$$

where, i refers to the i^{th} value of the velocity (U) and pressure drop (Δp). The uncertainty associated with the constant a is,

$$\Delta a = \sqrt{\sum \left(\frac{\partial a}{\partial U_i} \Delta U_i\right)^2 + \sum \left(\frac{\partial a}{\partial \Delta p_i} \Delta(\Delta p)_i\right)^2}, \tag{10}$$

where ΔU and $\Delta(\Delta p)$ are now the uncertainties in the velocity and pressure drop. The velocity at the midpoint of the channel cross-sectional area U_c is calculated as

$$U_c = \sqrt{2(P_{\text{stag}} - P_{\text{stat}})/\rho} \tag{11}$$

The mean velocity of air-flow in the rectangular channel, U_m was measured at various positions in the channel cross-section, and thus was determined by an area weighted-average correlation with U_c.

$$U_m = 0.9426 U_c - 0.5636 \tag{12}$$

The error in U_c is

$$\frac{\Delta U_c}{U_c} = \sqrt{\left(\frac{1}{2}\right)^2 \left[\left(\frac{\Delta P_{\text{stag}}}{P_{\text{stag}} - P_{\text{stat}}}\right)^2 + \left(\frac{\Delta P_{\text{stat}}}{P_{\text{stag}} - P_{\text{stat}}}\right)^2\right]} \tag{13}$$

Then, the error in U_m is calculated as

$$\frac{\Delta U_m}{U_m} = 0.9426 \times \frac{\Delta U_c}{U_c} \tag{14}$$

The error in pressure drop (Δp) is determined from the error in the pressures p_{in} and p_{out} across the sample by

$$\frac{\Delta(\Delta p)}{\Delta p} = \frac{\Delta(P_{in} - P_{out})}{P_{in} - P_{out}} = \sqrt{\left(\frac{\Delta P_{in}}{P_{in} - P_{out}}\right)^2 + \left(\frac{\Delta P_{out}}{P_{in} - P_{out}}\right)^2} \tag{15}$$

The uncertainty associated with $K (K = v_f/a)$ and f is estimated to be 5.8 and 3.9 %.

2.4.2 Effective Thermal Conductivity

Quantifying the thermal conductivity k using the present experimental setup is affected by the following parameters: q''_{net}, T_{e1}, T_{e2}, and H. With H fixed, the errors associated with the measurement of k_{e} may be estimated as (Coleman and Steele 2009)

$$\frac{\Delta k_{\text{e}}}{k_{\text{e}}} = \sqrt{\left(\frac{\Delta q''_{\text{net}}}{q''_{\text{net}}}\right)^2 + \left(\frac{\Delta T_{\text{e1}}}{T_{\text{e1}} - T_{\text{e2}}}\right)^2 + \left(\frac{\Delta T_{\text{e2}}}{T_{\text{e1}} - T_{\text{e2}}}\right)^2}, \tag{16}$$

where the error associated with the temperatures T_{e1} and T_{e2} due to film thermocouple calibration and resolution of the data acquisition device is estimated to be 0.2 °C. For the input heat flux q''_{net} measured by the film heat flux gage, the error stems mainly from signal readings by the multimeter and is estimated to be within 2.0 %. Overall, the uncertainty in the present measurement of effective thermal conductivity is estimated to be less than ±3.5 %.

2.4.3 Overall and Modified Heat Transfer Rate

The Nusselt number Nu_{av} is affected by the following parameters, q'', T_{w}, T_{∞}, k_{f}, and L. With L and k_{f} assumed to be constant, the errors associated with Nu_{av} are estimated as (Coleman and Steele 2009):

$$\frac{\Delta Nu_{\text{av}}}{Nu_{\text{av}}} = \sqrt{\left(\frac{\Delta q''}{q''}\right)^2 + \left(\frac{\Delta T_{\text{w}}}{T_{\text{w}} - T_{\infty}}\right)^2 + \left(\frac{\Delta T_{\infty}}{T_{\text{w}} - T_{\infty}}\right)^2} \tag{17}$$

The error associated with the temperatures T_{w} and T_{∞} measured by the thermocouples was estimated to be 0.2 °C. The minimum substrate temperature difference $(T_{\text{w}} - T_{\infty})$ was measured to be 5.3 °C at $q'' = 519\ \text{W/m}^2$. The error of q'' measured by the heat flux gage was estimated to be within 2 %. Consequently, the uncertainty in Nu_{av} was less than 6.4 %. It needs to be noted here that the errors associated with the average heat transfer coefficient h_{av} (Eq. (7)) can be also estimated by Eq. (17) with L and k_{f} assumed to be constant.

For the modified Nusselt numbers Nu_{m}, the effective thermal conductivity of porous core is considered (see Sect. 3.4), which leads to a propagation of errors in the modified Nusselt numbers Nu_{m}. Therefore, the errors associated with Nu_{m} are estimated as Coleman and Steele (2009):

$$\frac{\Delta Nu_{\text{m}}}{Nu_{\text{m}}} = \sqrt{\left(\frac{\Delta q''}{q''}\right)^2 + \left(\frac{\Delta T_{\text{w}}}{T_{\text{w}} - T_{\infty}}\right)^2 + \left(\frac{\Delta T_{\infty}}{T_{\text{w}} - T_{\infty}}\right)^2 + \left(\frac{\Delta k_{\text{e}}}{k_{\text{e}}}\right)^2} \tag{18}$$

With the propagated errors of effective thermal conductivity for porous core are estimated by Eq. (16), the total errors associated with Nu_{m} are estimated to be within 7.3 %.

3 Results and Discussions

3.1 Overall Natural Convection Heat Transfer Rate

Figure 4 displays the average heat transfer rate (Nu_{av}) as a function of heating power ($Ra_{q''}$) for WBK in both horizontal ($\theta = 0°$) and vertical ($\theta = 90°$) positions. For both positions, the average Nu_{av} number is greatly depended upon $Ra_{q''}$, showing an increment trend. As for a given $Ra_{q''}$ number, the average Nu_{av} number is increased with dimensionless sample

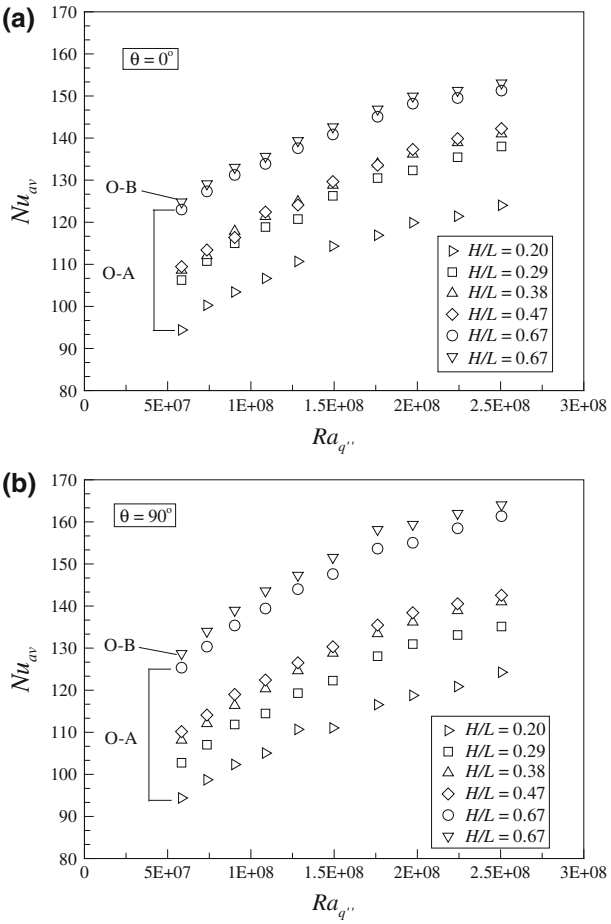

Fig. 4 Experimental heat transfer rate (Nu_{av} number) as a function of heat input ($Ra_{q''}$ number) for: **a** horizontal position, **b**vertical position

height (H/L). The sample (O-B orientation, $H/L = 0.67$) offers the most superior heat transfer performance among the samples and its average Nu_{av} number is found to be 2.35 times higher than smooth plate (Incropera et al. 2011) in the present $Ra_{q''}$ number range.

Wire-Woven Bulk Kagome differs from the conventional porous media, showing a strong anisotropy (see Fig. 1b–d). The anisotropy in structure is expected to result in the anisotropy feature in natural convection heat transfer. Anisotropic heat transfer was observed for WBK specimen under a given position (horizontally and vertically). For horizontal position, Nu_{av} for O-B orientation is approximately 7 % higher than that for O-A orientation, and this enhancement is further increased to 10 % when the WBK specimen is vertically positioned.

To squarely address the anisotropy on natural convection heat transfer, the intrinsically anisotropic feature of WBK is analyzed. Its anisotropic structure results in the anisotropic open area ratio (or (1-cross-sectional surface area density)) that is defined as the ratio of the projected void area to the whole area in the flow direction. The open area ratios of O-A and O-B are 0.75 and 0.62, respectively (or the cross-sectional surface area density for O-A and O-B are 0.25 and 0.38, respectively). A bigger cross-sectional surface area density, i.e., a

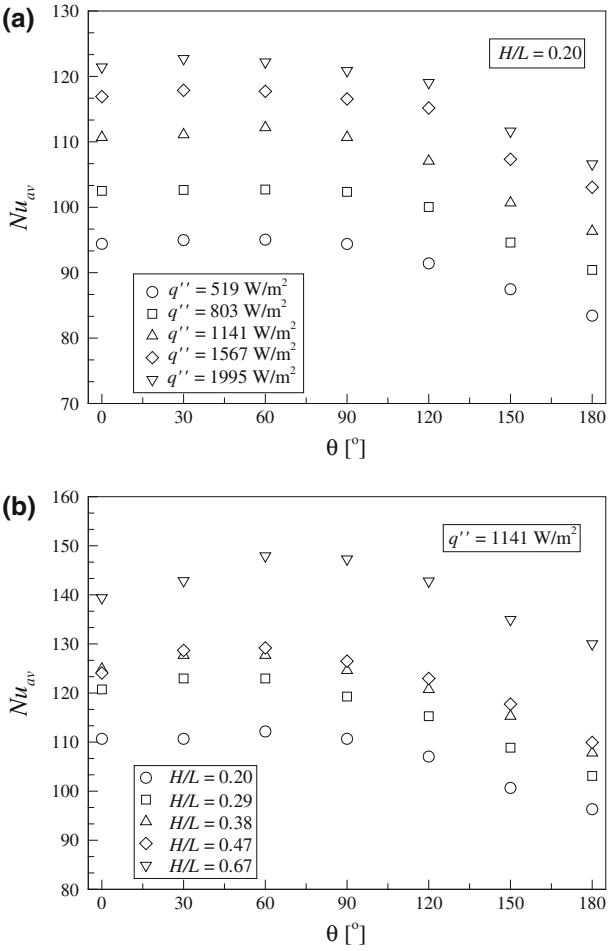

Fig. 5 Effect of inclination angle on heat transfer rate in O-A orientation: **a** for a given sample height with various heat fluxes; **b** for a given heat flux with various sample heights

larger upwind surface area causes a higher heat transfer between the fluid flow and the solid ligaments. Furthermore, there are additional ligaments in each pore for O-B orientation (see Fig. 1b, c). These ligaments disturb more flow and promote further flow mixing, leading to the observed higher natural convection from O-B than O-A in vertical position.

3.2 Optimal Inclination Angle

Given the different installation angles of electronic devices, the effect of inclination angle upon the thermal performance of heat sinks needs to be examined. Special care was taken to investigate the effects of the inclination angle on the average Nusselt number Nu_{av} concerning heat flux and sample height. Figure 5a demonstrates the effects of the inclination angle on the average Nu_{av} number for a given sample height ($H/L = 0.20$) with various heat fluxes. For a given heat flux, e.g., $q'' = 519$ W/m^2, the average Nu_{av} number is first increased then decreased with inclination angle, there being a peak around 60° (optimal inclination angle)

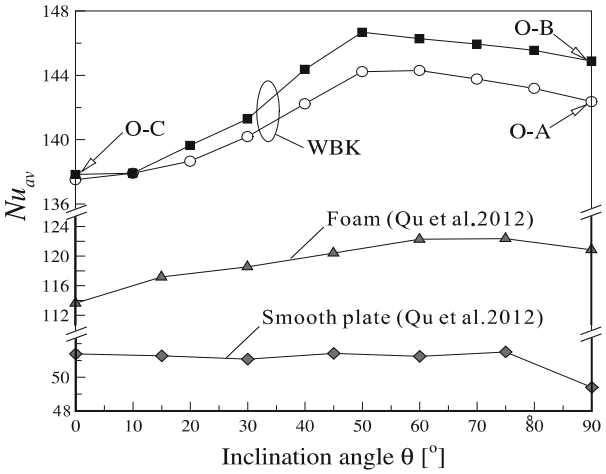

Fig. 6 Optimal inclination angle for smooth plate, metallic foams and WBK in the angle range of 0°–90°.

in association with maximum heat transfer rate during the inclination angle range (0°–180°). Similar trend was found in terms of optimal inclination angle at each heat flux, and this trend was more evident at a higher heat flux.

At a given heat flux ($q'' = 1141$ W/m^2), the variation in sample height under different inclination angles may result in the varied Nu_{av} number. Similar trend was found in terms of optimal inclination angle for various sample heights in Fig. 5b, which is in consistent with the observation for natural convection in tilted metallic foams (Qu et al. 2012; Al-Bahi et al. 2006). To address this issue, the average Nu_{av} number for a given WBK specimen ($H/L = 0.67$) was measured with a fine angle increment in the range of $0° - 90°$ (see Fig. 6). Qu and Al-Bahi (Qu et al. 2012; Al-Bahi et al. 2006) regarded the possible reason as the fact that the optimal inclination angle was associated with the lowest viscous force in metallic foams. However, it is observed from the experimental results that there exists an optimal inclination angle for heated smooth plate as well (see diamond marks in Fig. 6), which implying the physical understanding and fluid physics for the existence of optimal inclination angle have not been fully understood.

Thinning and thickening of thermal boundary layer on a smooth uniformly heated flat plate as a result of inclination have been accepted to be responsible for the existence of the maximum natural convection heat transfer coefficient between the two positions (horizontal and vertical positions). Considering a smooth plate heated on one side, the fluid is driven by the buoyancy force $\boldsymbol{F}$ that is the opposite direction to the gravity acceleration. Generally, the buoyancy force vector $\boldsymbol{F}$ has two components: they are normal / parallel to the smooth plate surface, named by $\boldsymbol{F}_1$ and $\boldsymbol{F}_2$. As the plate is inclined (0°–90°), the inclination results in the increase in parallel buoyancy force $\boldsymbol{F}_2$, from 0 to $\boldsymbol{F}$ sin θ, but the decrease in normal buoyancy force $\boldsymbol{F}_1$, from $\boldsymbol{F}$ to $\boldsymbol{F}$ cos θ, leading to an increased local parallel velocity and strengthened fluid replacement (by increased $\boldsymbol{F}_2$) but thickened boundary layer (by reduced $\boldsymbol{F}_2$). Considering the variation form in both of the two factors ($\theta = 0°–90°$), the overall heat transfer rate is first increased then decreased with inclination angle, leading to a speculated optimal inclination angle for the maximum natural convective heat transfer rate during the full inclination in smooth plate.

The extended surfaces attached to the smooth plate may influence the above-mentioned mechanism for the optimal inclination angle. The present WBK with highly conducting

ligaments and metallic foams is expected to reduce the optimal inclination angle due to the further thinning of thermal boundary layer caused by strengthened heat conduction. Figure 6 shows the average Nu_{av} number that varies with the inclination angle, for the WBK. As reference, the data for an copper foam and a smooth plate from Reference (Qu et al. 2012) is included where the heat flux is 1,149 W/m^2. The optimal angle exists for the WBK at $\theta = 50° - 60°$, for the Cu foam at $\theta = 60° - 70°$, and for the smooth plate at $\theta \sim 75°$. With the inclination of porous extended surfaces (i.e., WBK and Cu foam) from the horizontal position ($\theta = 0°$), the metallic ligaments of the two may cause a further thinning of a thermal boundary layer from the substrate. This may result in the smaller optimal inclination angle for the maximum natural convection heat transfer coefficient than the smooth plate.

Foams are aerodynamically isotropic. The fluid flow induced by buoyancy forces convects upwards opposite to the gravitational axis but experiences the same heat transfer area (blockage ratio) in the horizontal plane which is normal to the gravity direction and the same flow resistance per unit length (i.e., the identical permeability regardless of the inclination). Hence, the behavior of the overall heat transfer rate resembles smooth plate. On the other hand, WBK is aerodynamically anisotropic, implying an anisotropic heat transfer rate during the different inclining processes (O-C-A and O-C-B). A higher Nu_{av} number is observed for O-C-B than O-C-A curve, especially for the two typical positions: optimal angle and vertical position, as well.

3.3 Effect of Sample Height

The height of sample is expected to affect the heat transfer area and the viscous drag subjected to natural convection. For a given porous structure with fixed porosity and pore density (PPI), e.g., WBK for an orientation, the effective thermal conductivity and permeability can be regarded as unchanged, leading to the unchanged heat conduction through tortuous ligaments and form drag experienced by buoyant fluid. Hence, the increase in sample height results in the enlargement in the heat transfer surface area and associated increased viscous drag. The heat transfer performance increased with the sample height H/L, varied from 0.20 to 0.67 because of the obvious surface extension, which exceeded the negative effect of increased viscous drag (see Fig. 7). The increasing trend became sharper at higher aspect ratio ($H/L > 0.5$) because increased heat transfer surface area to enhance natural convection became more apparent. The viscous drag is influenced by inclination angle and the viscous drag effect is comparatively significant with smaller H/L. Hence, the effect of inclination angle on Nu_{av} becomes substantial at large H/L.

3.4 Comparison with Bejan's Scale Analysis

The obtained Nusselt number in the vertical orientation of the present experimental study was compared with Bejan's analytical solution (Bejan 2003) . The solution was applied to a vertical impermeable wall embedded in a saturated porous media and obtained by scale analysis on the natural convection boundary layer near the wall. The modified Nusselt numbers Nu_{m} and Darcy-modified Rayleigh numbers Ra_{m} are defined in Eqs. (19a) and (19b) as

$$Nu_{\mathrm{m}} = \frac{h_{\mathrm{av}} L}{k_{\mathrm{e}}} \tag{19a}$$

$$Ra_{\mathrm{m}} = \frac{g\beta q'' L^2 K}{\alpha_{\mathrm{e}} \nu_{\mathrm{f}} k_{\mathrm{e}}}, \tag{19b}$$

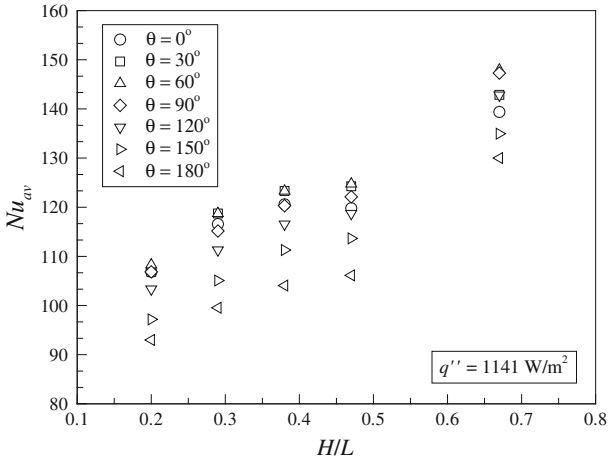

Fig. 7 Effect of sample height on the Nuav number in terms of various inclination angles ranging from 0° to 180° in O-A orientation

where α_e and k_e are the effective thermal diffusivity and thermal conductivity of air-saturated WBK specimen, K is the hydraulic permeability. Using these modified dimensionless numbers, Bejan proposed the scale analysis for the heat transfer rate Nu_m with uniform heat flux condition as

$$Nu_m = C Ra_m^{1/3}, \tag{20}$$

where the coefficient C may have different values for different porous media. The comparative results of Nu_m number obtained from the present experimental measurement of O-A orientation with the scale analysis-based analytical solution from Bejan (Bejan 2003) are plotted and shown in Fig. 8. The present measurement data show an increment trend for modified Nusselt number Nu_m with Darcy-modified Rayleigh number Ra_m, achieving good agreement (deviation within 6.5 %) with Bejan's scale analysis. The constant coefficient C in Eq. (20) takes the value of 0.225 and 0.241 for O-A and O-B orientation respectively.

3.5 Comparison with Open-Cell Metal Foams

Natural convection heat transfer in porous media is known to be influenced by many parameters as

$$h_{av} = f\left(K, k_e, \frac{A}{V}...\right), \tag{21}$$

where K is the permeability, k_e is the effective thermal conductivity and A/V is the surface area per unit volume (also called the specific surface area). To separate the contribution of each parameter, a systematic evaluation is required.

3.5.1 Effective Thermal Conductivity

Based on UC analysis, Yang et al. (Yang et al. 2013, 2014b, 2013) proposed an analytical model to estimate the effective thermal conductivity of highly porous heterogeneous materials

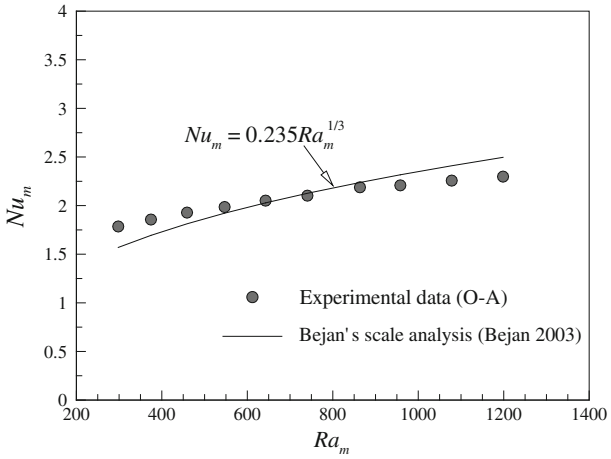

Fig. 8 Comparisons of Nu_{m} number obtained from the present experimental measurement with the scale analysis-based analytical solution from Bejan (Bejan 2003)

which shows good agreement with high porosity metallic foams. By exploiting this model, the effective thermal conductivity of high porosity WBK in O-C orientation is obtained by

$$\frac{k_{\mathrm{e}}}{k_{\mathrm{s}}} = \left(\frac{H_{\mathrm{c}}}{A_0}\right) \Big/ \left(\int_0^{H(s)} \frac{1}{A_{\mathrm{L}}(s)} ds \right), \tag{22}$$

where A_0 and H_{c} are the heat transfer area and thickness of the UC (see Fig. 9), the heat transfer length via the tortuous ligaments in the UC can be calculated as

$$\int_0^{H(s)} \frac{1}{A_{\mathrm{s}}} ds = \frac{8L_{\mathrm{d}}}{3\pi d^2} \tag{23}$$

With the relative density ($\rho^* = 1 - \varepsilon$) determined as

$$\rho^* = 1 - \varepsilon = \frac{3\pi d^2}{4\sqrt{2}L_{\mathrm{d}}^2} \tag{24}$$

the effective thermal conductivity of WBK in O-C orientation can be predicted as

$$\frac{k_{\mathrm{e}}}{k_{\mathrm{s}}} = \frac{1}{3}(1 - \varepsilon) \tag{25}$$

which is exactly *the same* mathematical formula as that for high porosity metallic foams, implying that WBK and metallic foams have *the same* conductivity value with a given porosity even if the porous structure differs. It needs to note that the effective thermal conductivity is greatly dependent on the anisotropy of the WBK. At present, only the O-C orientation is analyzed due to the place where the plate is sintered.

Open-cell metallic foams are typically fabricated by direct foaming, precision casting, and seepage casting. The former two methods can produce foams with solid ligaments, but seepage casting produces foams with hollow ligaments (Bhattacharya et al. 2002), leading to a further reduced effective thermal conductivity compared with foams having solid ligaments

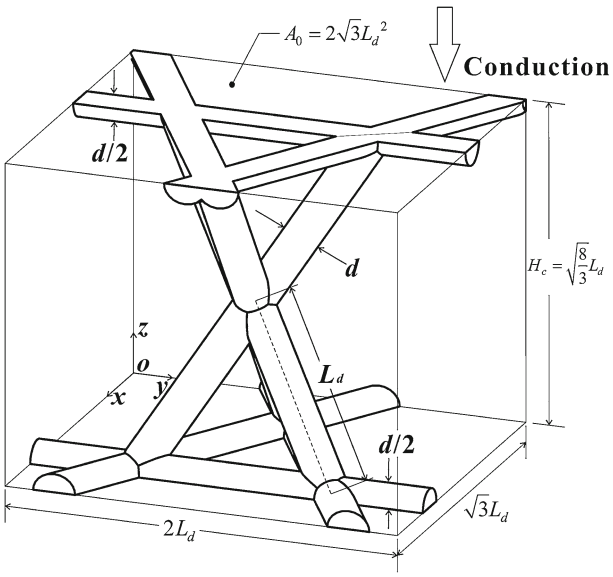

Fig. 9 Unit cell model of a non-twisted Kagome structure having a uniform diameter of circular ligaments, d and lateral length, L_d

for a given porosity. Zhao et al. (Zhao et al. 2004) considered the contribution of hollow ligaments in the overall effective thermal conductivity of bulk steel alloy FeCrAlY foams by introducing an inner-to-outer radius ratio of the hollow struts as

$$k_{\mathrm{e,h}} = k_\mathrm{e}(1-r)^2, \tag{26}$$

where $k_{\mathrm{e,h}}$ is the effective thermal conductivity of foams with hollow ligaments, k_e is that with solid ligaments and the same porosity, r is the inner-to-outer radius ratio of the hollow struts. Qu's foams (Qu et al. 2012) are inner hollow, so their effective thermal conductivity should be estimated by Eqs. (25) and (26).

Figure 10 displays the comparison of effective thermal conductivity for wire-woven bulk Kagome with metallic foams having solid and hollow ligaments. The effective thermal conductivity of Al foams having solid ligaments and WBK obtained from the present experimental measurement and open literature (Yang et al. 2014b,Yang et al. 2014a) lies in the same curve (analytical model, Eq. (25)), which is in accordance with the previous analysis. As for foams having hollow ligaments, the analytically predicted effective thermal conductivity is much lower than that having solid ligaments, see Fig. 10.

3.5.2 Permeability

Permeability K is a property of porous media that describes the easiness of a fluid saturating the media through a void space. It, therefore, depends on the intrinsic topology of individual porous media. To quantify the permeability, pressure drop across the WBK was measured subject to fully developed and steady-state flow and the pressure drop data as a function of the mean flow velocity were manipulated. The measured pressure drop for the two selected orientations, O-A and O-B are plotted against the mean flow velocity U_m in Fig. 11. The

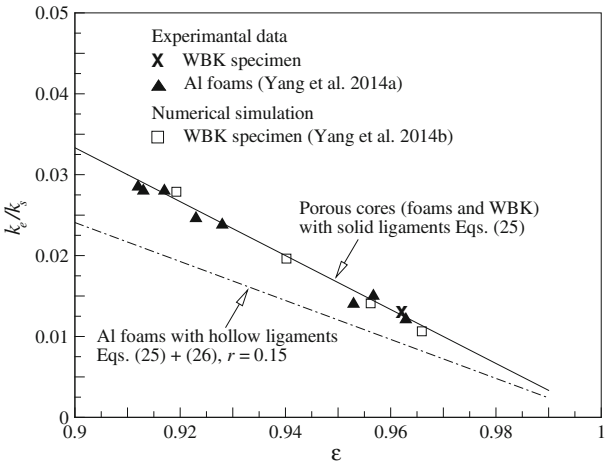

Fig. 10 Comparisons of effective thermal conductivity for wire-woven bulk Kagome with metallic foams having solid and hollow ligaments

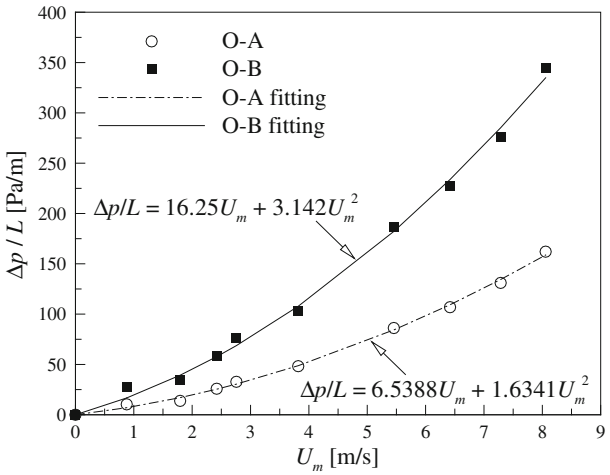

Fig. 11 Pressure drop per unit length across a WBK sandwich plotted as a function of inlet mean flow velocity U_{m}

pressure drop increases with increasing the mean velocity in a quadratic fashion and is empirically correlated as

$$\Delta p/L = 6.5388U_{\mathrm{m}} + 1.6341U_{\mathrm{m}}^2,\ R^2 = 0.99887 \tag{27a}$$

$$\Delta p/L = 16.25U_{\mathrm{m}} + 3.142U_{\mathrm{m}}^2,\ R^2 = 0.99808 \tag{27b}$$

The constants, a and b in Eq. (2) were then estimated to be $K_{\mathrm{O-A}} = 8.45 \times 10^{-6}$ and $K_{\mathrm{O-B}} = 1.36 \times 10^{-6}$, and $f_{\mathrm{O-A}} = 0.01194$ and $f_{\mathrm{O-B}} = 0.00164$, respectively.

Permeability for fibrous porous media is analytically and experimentally investigated by many researchers (Bhattacharya et al. 2002; Plessis et al. 1994; Paek et al. 2000; Moreira et al. 2004). Among them, the experimental data measured by Bhattacharya et al. (Bhattacharya et al. 2002) may be considered as bench mark for metallic foams. In the present

study, the permeability value of both copper and aluminum foams is from Bhattacharya et al. Bhattacharya et al. (2002). They argued that the permeability of foams is significantly increased with the decrease in pore density (or increase in pore size). The permeability of the present WBK sample has the pore density of about 2 pores per inch (PPI) and the porosity of $\varepsilon = 0.962$ for the both selected orientations i.e., O-A and O-B, is found to be 10.57 and 4.24 times higher than that of an Al foam with 5 PPI, $\varepsilon = 0.973$ ($K = 2.7 \times 10^{-7}$) (Calmidi and Mahajan 2000). It should be noted that one permeability value represents a given isotropic porous medium regardless of its orientation, whereas different orientations have its own permeability if the medium of interest is anisotropics such as WBK.

3.5.3 Specific Surface Area

It has been reported that at high porosity ranges, $\varepsilon > 0.9$, the specific surface area of foams may be expressed as (Calmidi and Mahajan 2000):

$$\frac{A}{V} = \frac{1.18\sqrt{3\pi(1-\varepsilon)}}{d_{\mathrm{p}}(1-e^{-(1-\varepsilon)/0.04})}, \tag{28}$$

where d_{p} is the pore diameter of foams. For the WBK, it may be expressed as

$$\frac{A}{V} = \frac{4}{d}(1-\varepsilon), \tag{29}$$

where d is the diameter of circular wires (ligaments). For typical metallic foams with a porosity of 0.973 and a pore density of 5PPI, A/V is estimated to be 357 $\mathrm{m}^2/\mathrm{m}^3$; while for the present WBK specimen (wire diameter is 0.98 mm, porosity is 0.962), A/V is estimated as 155 $\mathrm{m}^2/\mathrm{m}^3$.

3.5.4 Comparisons of Heat Transfer Rate

Figure 12 compares the average heat transfer coefficient h_{av} of the WBK and Cu and Al foams where the both are attached to a vertical plate, made of Aluminum and subject to natural convection. To systemically investigate those porous cores, experimental data from both open literature and the present measurements are compared. Due to the experimental data of heat transfer rate for foams in open literature are processed in the form of Rayleigh number under constant temperature thermal boundary (Ra_{T} number) and the heating substrate differs from each other, a comparable base was set. We transferred the present measurement data into Ra_{T} number and used parameters without length scale as the base for comparison.

For a given Ra_{T} number, the heat transfer rate h_{av} of the WBK is 13 % higher than that of the Al foams compared. For a similar porosity of the WBK ($\varepsilon = 0.962$) and the Al foam ($\varepsilon = 0.9586$, 40PPI), a 62 % more heat can be removed by the WBK. The possible reasons are discussed as follows. For a similar porosity Al metal foams have larger specific surface area than Al WBK while the two have the same effective thermal conductivity. But, WBK shows a higher h_{av} than metal foams. As discussed previously, the permeability of the present WBK sample is 10.57 and 4.24 times higher than that of an Al foam with 5 PPI, $\varepsilon = 0.973$ ($K = 2.7 \times 10^{-7}$) (Calmidi and Mahajan 2000). This means more cooling flow convects through WBK resulting in better natural convection heat transfer as observed in Fig. 12. Although the metal foams have the higher specific surface area, there exist larger thermally inactive regions ("dead area") on Al foam's sharp ligaments than WBK whose ligaments are circular. This argument is further supported by the data in Fig. 12 showing a

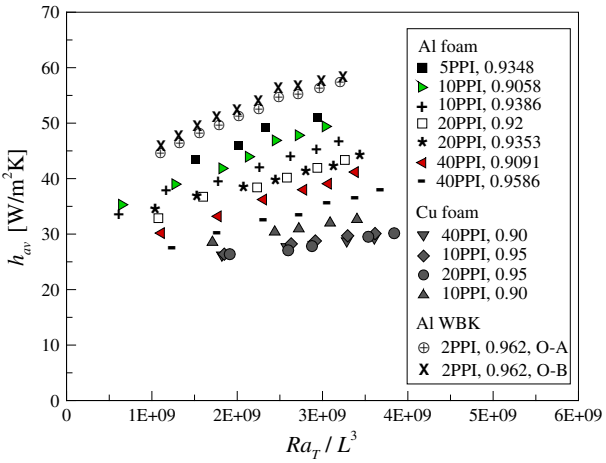

Fig. 12 Comparisons of the average heat transfer coefficient h_{av} of WBK with metallic foams (Bhattacharya and Mahajan 2006; Qu et al. 2012), attached to a uniformly heated vertical plate

further reduction of the heat transfer coefficient when the specific surface area continues to increase (due to a further increased pore density). Among the Al foam data in Fig. 12, the heat transfer coefficient is reduced by 19.3 % when the specific area density is increased by 298.7 % and when the pore density is increased from 10 PPI to 40 PPI for the foams with a porosity of ~ 0.90.

For Cu foams, a lower heat transfer rate is "strangely" observed than Al foams. That is due to the lower effective thermal conductivity resulted from the hollow ligaments of Cu foams, which implies that the effective thermal conductivity plays a vital role in conducting heat from the substrate where thermal load is applied to the extended surface for cooling.

In summary, it can be therefore concluded that with similar effective thermal conductivity and porosity, higher natural convection heat transfer can be achievable if less flow resistance exists as in WBK compared to metal foams. The WBK core has a relatively bigger pore diameter (smaller pore density, $\sim$ 2PPI) than that of typical metal foams, leading to the less flow resistance to natural convection than that for the metal foams. The higher permeability means the smaller pressure drop when the fluid flows across the porous media, implying a higher local flow velocity. With similar permeability and porosity, a higher effective thermal conductivity should be guaranteed to keep a stronger thermal transport from heat source to extended surface. Specific surface area may contribute to enhancing heat transfer if stronger heat conduction (higher k_e) and more coolant fluid (higher K) are guaranteed.

4 Conclusions

Natural convection heat transfer in a wire-woven bulk Kagome (WBK) was experimentally characterized and the results are compared with typical engineering porous foams. The present findings are summarized as follows:

(1) There exists an optimal inclination angle for heated smooth plate in association with the maximum natural convection heat transfer rate due mainly to the thinning and thickening of thermal boundary layer. The optimal inclination angle becomes smaller with conducting porous media sintered on a smooth plate owing mainly to a further thinning of a thermal boundary layer from the substrate caused by highly conducting metallic ligaments.

(2) The overall heat transfer rate shows a strong dependence on the anisotropy of the WBK: the average Nusselt number in the more closed orientation (O-B) is consistently (slightly) higher than that in the more open orientation (O-A), due mainly to a higher cross-sectional surface area of the more closed orientation (O-B).
(3) Compared with typical porous media e.g., metallic foams with a similar porosity (~ 0.96), WBK exhibits a 62 % enhancement in the heat transfer rate h_{av} due to a much greater mass of cooling fluid with a higher local velocity resulted from a higher permeability.
(4) For porous media having a relatively high permeability e.g., WBK in the present study, heat transfer area seems significant: heat transfer rate for O-B is higher than O-A orientation. While for those having a relatively low permeability (metallic foam), flow resistance (permeability) governs the overall heat transfer: heat transfer rate is significantly increased by enlarging pore size (increasing permeability).

Acknowledgments This work was supported by the National 111 Project of China (B06024), the National Basic Research Program of China (2011CB610305) and the National Natural Science Foundation of China (51206128).

References

Al-Bahi, A., Al-Hazmy, M., Zaki, G.M.: Natural convection in a tilted rectangular enclosure with a single discrete heater. JKAU. Eng. Sci **16**(2), 141–168 (2006)
Antohe, B.V., Lage, J.L., Price, D.C., Weber, R.M.: Experimental determination of permeability and inertia coefficients of mechanically compressed aluminum porous matrices. J. Fluids Eng. **119**(2), 404–412 (1997)
Beavers, G.S., Sparrow, E.M.: Non-Darcy flow through fibrous porous media. J. Appl. Mech. **36**, 711 (1969)
Bejan, A.: Simple methods for convection in porous media: scale analysis and the intersection of asymptotes. Int. J. Energy Res. **27**(10), 859–874 (2003)
Bhattacharya, A., Calmidi, V.V., Mahajan, R.L.: Thermophysical properties of high porosity metal foams. Int. J. Heat Mass Transf. **45**(5), 1017–1031 (2002)
Bhattacharya, A., Mahajan, R.L.: Metal foam and finned metal foam heat sinks for electronics cooling in buoyancy-induced convection. Trans. Am. Soc. Mech. Eng. J. Electr. Packag. **128**(3), 259–266 (2006)
Calmidi, V.V., Mahajan, R.L.: Forced convection in high porosity metal foams. J. Heat Transf. **122**(3), 557–565 (2000)
Chiras, S., Mumm, D.R., Evans, A.G., Wicks, N., Hutchinson, J.W., Dharmasena, K., Wadley, H.N.G., Fichter, S.: The structural performance of near-optimized truss core panels. Int. J. Solids Struct. **39**(15), 4093–4115 (2002)
Coleman, H.W., Steele, W.G.: Experimentation, Validation, and Uncertainty Analysis for Engineers. Wiley, New York (2009)
Du Plessis, P., Montillet, A., Comiti, J., Legrand, J.: Pressure drop prediction for flow through high porosity metallic foams. Chem. Eng. Sci. **49**(21), 3545–3553 (1994)
Evans, A.G., Hutchinson, J.W., Fleck, N.A., Ashby, M.F., Wadley, H.N.G.: The topological design of multifunctional cellular metals. Prog. Mater. Sci. **46**(3), 309–327 (2001)
Hoffmann, F., Lu, T.J., Hodson, H.P.: Heat transfer performance and pressure drop of Kagome core metal truss panels. In: Proceedings of the 8th UK national heat transfer conference, Oxford. 9–10 Sept 54 (2003)
Hyun, S., Karlsson, A.M., Torquato, S., Evans, A.G.: Simulated properties of Kagomé and tetragonal truss core panels. Int. J. Solids Struct. **40**(25), 6989–6998 (2003)
Incropera, F.P., Lavine, A.S., DeWitt, D.P.: Fundamentals of Heat and Mass Transfer. Wiley, New York (2011)
Joo, J.-H., Kang, B.-S., Kang, K.-J.: Experimental studies on friction factor and heat transfer characteristics through wire-woven bulk Kagome structure. Exp. Heat Transf. **22**(2), 99–116 (2009)
Joo, J.-H., Kang, K.-J., Kim, T., Lu, T.J.: Forced convective heat transfer in all metallic wire-woven bulk Kagome sandwich panels. Int. J. Heat Mass Transf. **54**(25), 5658–5662 (2011)
Joseph, D.D., Nield, D.A., Papanicolaou, G.: Nonlinear equation governing flow in a saturated porous medium. Water Resour. Res. **18**(4), 1049–1052 (1982)
Kang, K.-J.: A wire-woven cellular metal of ultrahigh strength. Acta Mater. **57**(6), 1865–1874 (2009)

Kim, T., Hodson, H.P., Lu, T.J.: Fluid-flow and endwall heat-transfer characteristics of an ultralight lattice-frame material. Int. J. Heat Mass Transf. **47**(6), 1129–1140 (2004a)
Kim, T., Hodson, H.P., Lu, T.J.: Contribution of vortex structures and flow separation to local and overall pressure and heat transfer characteristics in an ultralightweight lattice material. Int. J. Heat Mass Transf. **48**(19), 4243–4264 (2005)
Kim, T., Zhao, C.Y., Lu, T.J., Hodson, H.P.: Convective heat dissipation with lattice-frame materials. Mech. Mater. **36**(8), 767–780 (2004b)
Lee, Y.-H., Lee, B.-K., Jeon, I., Kang, K.-J.: Wire-woven bulk Kagome truss cores. Acta Mater. **55**(18), 6084–6094 (2007)
Montgomery, D.C.: Design and Analysis of Experiments, vol. 7. Wiley, New York (1997)
Moreira, E., Innocentini, M., Coury, J.: Permeability of ceramic foams to compressible and incompressible flow. J. Eur. Ceram. Soc. **24**(10), 3209–3218 (2004)
Paek, J., Kang, B., Kim, S., Hyun, J.: Effective thermal conductivity and permeability of aluminum foam materials1. Int. J. Thermophys. **21**(2), 453–464 (2000)
Qu, Z.G., Wang, T.S., Tao, W.Q., Lu, T.J.: Experimental study of air natural convection on metallic foam-sintered plate. Int. J. Heat Fluid Flow **38**, 126–132 (2012)
Vafai, K., Tien, C.L.: Boundary and inertia effects on convective mass transfer in porous media. Int. J. Heat Mass Transf. **25**(8), 1183–1190 (1982)
Yan, H.B., Zhang, Q.C., Lu, T.J., Kim, T.: The modification of a primary convective flow by a new periodic cellular core in a sandwich panel. Int. J. Heat Mass Transf. **49**, 3313–3324 (2013)
Yang, X.H., Bai, J.X., Kang, K.-J., Lu, T.J., Kim, T.: Effective thermal conductivity of wire-woven bulk Kagome sandwich panels. Theor. Appl. Mech. Lett. (2014a)
Yang, X.H., Bai, J.X., Yan, H.B., Kuang, J.J., Lu, T.J., Kim, T.: An analytical unit cell model for the effective thermal conductivity of high porosity open-cell metal foams. Transp. Porous Media **9**, 1–24 (2014b)
Yang, X.H., Kuang, J.J., Lu, T.J., Han, F.S., Kim, T.: A simplistic analytical unit cell based model for the effective thermal conductivity of high porosity open-cell metal foams. J. Phys. D **46**(25), 255302 (2013a)
Yang, X.H., Lu, T.J., Kim, T.: Thermal stretching in two-phase porous media: physical basis for Maxwell model. Theor. Appl. Mech. Lett. **3**(2), 021011 (2013b)
Zhao, C., Lu, T., Hodson, H., Jackson, J.: The temperature dependence of effective thermal conductivity of open-celled steel alloy foams. Mater. Sci. Eng. A **367**(1), 123–131 (2004)
Zok, F.W., Waltner, S.A., Wei, Z., Rathbun, H.J., McMeeking, R.M., Evans, A.G.: A protocol for characterizing the structural performance of metallic sandwich panels: application to pyramidal truss cores. Int. J. Solids Struct. **41**(22), 6249–6271 (2004)